Published in final edited form as:
Evol Biol. 2009 March ; 36(1): 19–36. doi:10.1007/s11692-009-9056-9.

Comparison of Mandibular Phenotypic and Genetic Integration between Baboon and Mouse

Katherine E. Willmore,
Department of Anthropology, Pennsylvania State University, 409 Carpenter Building, University Park, PA 16802, USA

Charles C. Roseman,
Department of Anthropology, University of Illinois, 109 Davenport Hall, 607 S. Matthews Ave., Urbana, IL 61801, USA

Jeffrey Rogers,
Department of Genetics, Southwest Foundation for Biomedical Research, San Antonio, TX 78245-0549, USA

James M. Cheverud, and
Department of Anatomy and Neurobiology, Washington University Medical School, 660 Euclid Ave., St. Louis, MO 63110, USA

Joan T. Richtsmeier
Department of Anthropology, Pennsylvania State University, 409 Carpenter Building, University Park, PA 16802

Katherine E. Willmore: kew20@psu.edu; Charles C. Roseman: croseman@uiuc.edu; Jeffrey Rogers: jr13@bcm.tmc.edu; James M. Cheverud: cheverud@pcg.wustl.edu; Joan T. Richtsmeier: jta10@psu.edu

Abstract

In this study we compare patterns of mandibular integration between mice and baboons using both phenotypic and quantitative genetic data. Specifically, we test how well each species fits with the mosaic model of mandibular integration suggested by Atchley and Hall (Biol Rev Camb Philos Soc 66:101–157, 1991) based on developmental modules. We hypothesize that patterns of integration will be similar for mice and baboons and that both species will show strong integration within developmental modules and weaker integration between modules. Corresponding landmark data were collected from the hemi-mandibles of an advanced intercross mouse sample ($N = 1239$) and mandibles from a baboon sample of known pedigree from the Southwest Foundation for Biomedical Research ($N = 430$). We used four methods of analysis to quantify and compare the degree of mandibular integration between species including two methods based on a priori assumptions, and two a posteriori analyses. We found that patterns of integration are broadly similar for baboon and mouse mandibles, with both species displaying a modular pattern of integration. While there is a general trend of similarity in integration patterns between species, there were some marked differences. Mice are strongly correlated among distances within the coronoid process and the incisive alveolar region, whereas baboons are strongly integrated within the condylar process. We discuss the potential evolutionary implications of the similar patterns of integration between these species with an emphasis on the role of modularity.

Correspondence to: Katherine E. Willmore, kew20@psu.edu.

Electronic supplementary material The online version of this article (doi:10.1007/s11692-009-9056-9) contains supplementary material, which is available to authorized users.

Keywords

Integration; Mandible; Mammalian; Modularity

Introduction

To understand the development, function and evolution of a morphological trait, we must understand how the trait fits within its broader structural context and its relationship with other component parts of the organism. Morphological integration is the study of these relationships between morphological traits and describes the interdependence, developmental or functional, of two or more structures. The aim of our study is to compare patterns of mandibular morphological integration between baboons and mice. Comparing patterns of integration between two such diverse species allows us to determine the relative impact of differing developmental programs and differing functional demands on the overall pattern of morphological integration of the mandible.

Olson and Miller's 1958 publication *Morphological Integration* introduced the concept, and laid out a methodology for the study of morphological integration. The theoretical underpinnings of morphological integration was not their largest contribution as these were incorporated into biology by holists such as Schmaulhausen and van der Klaauw. Instead, Olson and Miller's contribution was methodological as they demonstrated how correlation coefficients could be used to measure functional and developmental integration. A similar concept was independently advanced in Russia under the term correlation Pleiades (Berg 1960). As with morphological integration, correlation Pleiades are based on the correlation between a set of quantitative characters and the relative absence, or reduced magnitude, of correlation between other sets of quantitative traits.

The theoretical aspects of morphological integration were furthered by a series of studies conducted by Cheverud (1982, 1995, 1996) whereby integration was put within a quantitative genetics framework. Cheverud (1996) expanded on Olson and Miller's concept of integration at the individual level to also include a genetic level of integration and evolutionary integration. Individual integration refers to the functional and developmental relationships among parts, whereas genetic integration refers to the coinheritance of traits due to pleiotropy and/or linkage disequilibrium. The coinheritance of traits allows for the coordinated evolution of those traits which are integrated at the evolutionary level.

While the concept of morphological integration describes the association among parts, the concept of modularity emphasizes the dissociability of parts (Needham 1933). Generally, a module is a suite of characters that are more tightly integrated with one another than they are with other characters, and operate largely independently of other characters (Wagner 1996; Gass and Bolker 2002; Schlosser and Wagner 2004). Integration and modularity are strongly related concepts; essentially, modularity is nested integration (Willmore et al. 2007). For example, if we look at the mammalian mandible (or hemi-mandible) we can describe it as an integrated whole which functions primarily to masticate food. The mandible is also thought to be comprised of several developmental modules that correspond to separate cellular condensations of development, and different functional modules that correspond loosely to areas of muscle insertion and tooth eruption. Each of these modules makes a unique contribution to mastication (Atchley and Hall 1991). These various perspectives demonstrate how a single structure can be considered an integrated whole according to a specific set of criteria, or be decomposed into several modules using a different set of criteria. This idea of 'nearly decomposable systems' was first emphasized by Simon (1962), who suggested that integration is not absolute but is a matter of degrees. Here we add that it is a matter of focus,

a matter of the questions being asked by the investigator. That is, modules are not perfectly nested; there may be overlap between them based either on the criteria that drive the research question, or on a yet undiscovered criterion. Therefore, we must strive to understand all of the possible relationships among traits; some of these relationships are partially known to us and we can empirically test their strength, while others are currently unknown and may or may not be revealed to us a posteriori through studies of integration.

In this study we compare patterns of both phenotypic and genetic integration of baboon and mouse mandibles. Specifically, we compare the right hemi-mandible of mice with the right side of the baboon mandible. Two methods of analyses used here adopt an a posteriori approach that does not incorporate assumptions of developmental, functional or genetic relationships among traits within the mandible. The other two methods used here adopt a priori assumptions based on the developmental divisions of the mandible suggested by Atchley and Hall (1991) who argued that the mandible is divided into six mesenchymal condensations with different cellular properties, each being a primary determinant of adult mandibular morphology across mammals. This view of mandibular development is consistent with the recent finding that cellular proliferation in the mouse mandible generates its macroscopic growth (Ramaesh and Bard 2003) and presumably its eventual shape. The six mesenchymal condensations form a molar and an incisive alveolar module, and four ascending ramus modules including the condylar, coronoid, and angular processes and the masseteric region. On the basis of landmark data available, we consider five of these modules, excluding the masseteric region (Fig. 1). While the autonomy of these modules was hypothesized using specific developmental criteria, each module makes a distinct contribution to the functional requirement of mastication. The coronoid process serves as an attachment site for the temporalis muscle, the condylar process is an attachment site for the lateral pterygoid muscle and contributes to the temporomandibular joint, and the angular process serves as an attachment site for the masseter and medial pterygoid muscles (Atchley and Hall 1991; Cheverud 2004). The size and shape of these processes are dependent on the function of the muscles that attach to them (Washburn 1947). Similarly, both alveolar modules are dependent on their interactions with the teeth embedded within them and the stresses placed on these teeth (Atchley and Hall 1991; Cheverud 2004). Therefore, while these proposed modules were initially based on developmental commonalities of specific cellular condensations, they are also influenced by functional interactions.

Following Atchley and Hall's (1991) argument, we hypothesize that patterns of mandibular integration will be similar in both baboons and mice, and will fit the modular pattern they described based on different cellular condensations. While Atchley and Hall (1991) used a rodent model to formulate their argument of mandibular integration, they suggested that this pattern would be found across mammals. Certainly, several studies involving mouse models have confirmed the modular pattern of mandibular integration suggested by Atchley and Hall (Atchley et al. 1985; Cheverud et al. 1991; Leamy 1993; Cheverud et al. 1997; Mezey et al. 2000; Ehrich et al. 2003; Klingenberg et al. 2003; Klingenberg et al. 2004). And similar patterns of integration have been found across a wide variety of mammalian species for a number of cranial traits (Marroig and Cheverud 2001; Goswami 2006; Mitteroeker and Bookstein 2008) suggesting that patterns of mandibular integration may be consistent across mammals.

Our aim is to gain a greater understanding of how developmental and functional factors influence mammalian mandibular morphology through a comparative study of two diverse mammalian species. We adopt a comparative approach to explore the influence that different potentially integrating factors have on mandibular morphology in species whose mandibles are morphologically and functionally distinct.

Materials and Methods

Composition of the Samples

Baboons—CT images of the skulls of 430 adult baboons (128 ♀ and 302 ♂; age range 6.04–33.7 years), from the Southwest Foundation for Biomedical Research (SFBR) in San Antonio, TX were used for these analyses. The baboons in the sample are *Papio hamadryas*, including pure-bred *P. h. anubis* (olive baboons), pure-bred *P.h. cynocephalus* (yellow baboons), *P.h. anubis–P.h. cynocephalus* hybrids of varying degrees, and other pure-bred subspecies (*P.h. hamadryas, P.h. papio*). The percentage of baboons in the sample from each subspecies is: 57% *P. h. anubis*, 36% *P.h. anubis–P.h. cynocephalus* hybrids, and 7% other subspecies (*P.h. cynocephalus, P.h. hamadryas, P.h. papio*). All of the animals used in this study are part of a known pedigree permitting quantitative genetic analyses. The baboons have ad libitum access to commercial monkey chow, and are housed outside in social groups. Dietary and housing conditions are the same for males and females. In accordance with the Guide for the Care and Use of Laboratory Animals (Council 1996) animal care personnel and staff veterinarians provide daily maintenance and health care to all animals. All procedures performed followed the policies established by the Southwest Foundation Institutional Animal Care and Use Committee.

Mice—Our mouse sample consists of 1239 adult mice (612 ♀, 627 ♂; age range 86–195 days) from the F_{10} generation of an advanced intercross line (Darvasi and Soller 1995), from an initial cross between LG/J and SM/J parental strains. LG/J and SM/J mice were obtained from The Jackson Laboratory (Bar Harbor, ME, USA) and had been selected to have large (LG/J) and small (SM/J) body sizes at 60 days (Goodale 1938, 1941; MacArthur 1944). Ten LG/J females were mated with 10 SM/J males to initiate the intercross producing F_1 mice that are completely heterozygous at variable loci (Norgard et al. 2008). F_1 mice were then randomly mated to produce an F_2 generation which was subsequently randomly mated to initiate an advanced intercross line of LG/J and SM/J mice, and repeated until the F_{10} generation (Darvasi and Soller 1995). Mice were mated, reared and prepared at Washington University in St. Louis following approved IACUC protocols. Details of the protocols used in raising the F_{10} mice are provided by Norgard et al. (2008).

Data Acquisition

Baboons—Baboon heads collected from the SFBR were macerated in a water bath. Medical computed tomography (CT) images were then acquired for each macerated skull including the articulated mandible at Washington University Mallinkrodt Institute of Radiology using a medical CT scanner (Siemens Medical Systems, Erlangen, Germany). Pixel sizes ranged from 0.20 to 0.61 mm depending upon the size of the specimen. Slice thickness was 0.75 mm. Three-dimensional reconstructions were produced from the CT image data and subsequently digitized to obtain 3D coordinates of biological landmarks using eTDIPS (http://www.cc.nih.gov/cip/software/etdips/). 3D coordinates of 23 mandibular landmarks, three midline and 10 bilateral, were recorded from each 3D reconstruction (Fig. 2, Table 1). We evaluated measurement error of landmark placement using established methods (Valeri et al. 1998). Measurement error was further minimized by landmarking each mandible twice, checking for gross errors such as side reversal, and using the average of the two data collection trials in analyses. From these landmark data we calculated 15 inter-landmark distances (Table 2) that are descriptive of the five developmental modules outlined by Atchley and Hall (1991) and correspond to linear distances measured on the mouse right hemi-mandibles (see below). We calculated repeatabilities for each distance using the method described by Lessells and Boag (1987), and these repeatabilities ranged from 0.61 to 0.99 with an average of 0.95.

Mice—Mouse skulls were macerated using dermestid beetles and from each skull, the right hemi-mandible was removed for use in our study. The lateral (buccal) aspect of the right hemi-mandible of each mouse was photographed using a digital camera. Twelve two-dimensional landmarks (Fig. 2, Table 1) were digitized from each photograph using the program ImageJ (version 1.38). Thirty mandibles were landmarked twice in order to calculate repeatability, the rest were landmarked once. Fifteen interlandmark distances were calculated that correspond to the distances calculated from the baboon data (Table 2). Repeatabilities calculated using the subset of 30 mice that were landmarked twice ranged from 0.61 to 0.98 with an average of 0.86.

Integration Analyses

Using the 15 homologous distances described above (Table 2), we compared morphological integration between mouse and baboon mandibles using four methods. The first two methods are based on a priori biological hypotheses of the developmental associations described by Atchley and Hall (1991). The third method uses partial correlations to explore the associations between different traits without a priori assumptions following the method discussed by Magwene (2001). A more direct comparison between species was performed via MIBoot (Cole 2002; Richtsmeier et al. 2006). MIBoot compares empiric correlation matrices directly by subtracting the correlation matrix for one sample from the correlation matrix of another sample producing a correlation difference matrix and the bootstrap is used to calculate confidence intervals for the correlation difference. Except for MIBoot which was used in the analysis of phenotypic data only, these analyses were used to compare integration between species for both phenotypic and quantitative genetic data.

Phenotypic Integration—All distance data were natural log-transformed and sexes were pooled for both mouse and baboon samples. To account for the effects of combining sexes and differently aged individuals, sex and age were used as covariates and the residual data were used for further analyses.

Our first test follows the method developed by Cheverud (Cheverud et al. 1989; Cheverud 1995; Marroig and Cheverud 2001) in which theoretical correlation (or covariance) matrices based on assumed functional and developmental associations are compared with empirical correlation matrices calculated from the data. A value of 1.0 was entered into any cell of the theoretical correlation matrix representing the relationship between two traits belonging to the same developmental module. A value of 0.0 was entered in any cell representing pairs of measures that belong to different modules. Consequently, our theoretical matrices assume absolute integration among measures within each of the five predefined modules (Fig. 1) and an absolute lack of integration between measures of the various modules. Additionally, we constructed a theoretical matrix that incorporated all five modules.

Matrix correlations between the observed correlation matrices for mice and baboons and the five theoretical correlation matrices were calculated using a Mantel's test with 1000 permutations using Microsoft Excel. This method allows us to separately compare how well baboon and mouse correlation matrices match the theoretical matrices, and therefore, indirectly compare the patterns of mandibular phenotypic integration between baboons and mice. It does not however, allow us to statistically compare the degree of integration between species for any of these regions.

Additionally, we calculated the average within-module correlation and the average between-module correlation for each of the five mandibular modules using the data from the phenotypic correlation matrices. We then calculated the difference of the average between-module correlation from the average within-module correlation, and used the permutation results from the Mantel's tests to assess the significance of differences in correlation. This

test is another way to look at the strength of correlations within developmental modules, but unlike the above tests using the theoretical matrices, it does not assume a complete lack of correlation among all other traits. Essentially, it gives a relative estimate of the strength of integration within a module compared with the strength of integration among all other traits not in the module.

To compare the degree of integration between baboons and mice, we calculated the variance of the eigenvalues for each of the five mandibular regions described above, and for the entire mandible following the method outlined by Wagner (1984, 1990). The premise of this integration index is that the eigenvalues of a correlation matrix describe the amount of variance associated with their corresponding eigenvectors. When there are only a few eigenvalues that are quite large in comparison to the rest of the eigenvalues, the traits are considered highly integrated. The relationship between a few large eigenvalues and high morphological integration is that the variation of the traits involved is confined to a smaller subspace in the overall multivariate phenotypic space (Wagner 1984, 1990). Variance of the eigenvalues from correlation matrices were calculated using the statistical software R and were compared between baboons and mice for each mandibular region. Each estimated variance of the eigenvalues was standardized by the number of traits by dividing the observed variance of the eigenvalues by the number of traits minus one (Pavlicev et al. 2009). Significance of differences in the variance of eigenvalues between species were calculated by bootstrapping each dataset using 1000 iterations; the statistical significance of the difference between two groups is calculated by the number of iterations in which the difference between the two resampled values exceeds zero, divided by the number of iterations.

Small sample sizes introduce a positive bias to the variance of the eigenvalues and given that our baboon sample is approximately a third of the size of our mouse sample, we correct for this bias. The correction is based on the assumption of no correlation between traits (Wagner 1984) and accounts for both sample size and the number of traits using the formula outlined in Cheverud (1989):

$$\mathrm{E}[V(\lambda)]=[\mathrm{M}-1]/\mathrm{N}$$

where M is the number of traits, N is the sample size and E[$V(\lambda)$] is the expected value of the variance of the eigenvalues. We use this correction to obtain a corrected observed variance of the eigenvalues for each sample as well as correcting the bootstrapped values for tests of significance. This correction was done for each comparison of the different developmental modules.

To further explore the patterns of mandibular integration in mice and baboons without a priori assumptions of expected developmental modules, we determined the conditional independence among the 15 distances using the method described by Magwene (2001). We calculated the partial correlation matrix for each sample; partial correlations are essentially the correlation of two variables after removing the effect of other controlling variables. To determine the conditional independence among mandibular distances we used the partial correlations and an information theoretic measure known as the edge exclusion deviance (EED):

$$\mathrm{EED}=-N\cdot ln\left(1-\rho^2_{ij\cdot[K]}\right),$$

where N is sample size and $\rho^2_{ij\cdot[K]}$ is the squared partial correlation of the ith and jth linear distances with all other traits held constant (Magwene 2001). Two traits are considered conditionally independent if they have an EED value of less than 3.84 which corresponds to $P = 0.05$, with $df = 1$, from the χ^2 distribution. Traits that have an EED >3.84 are conditionally dependent and therefore, are considered to be significantly integrated. To measure the edge strength (ES) of this conditional dependence between variables we used the formula:

$$\mathrm{ES} = -0.5 \cdot ln\left(1 - \rho^2_{ij\cdot[K]}\right),$$

where again, $\rho^2_{ij\cdot[K]}$ is the squared partial correlation of variables i and j, with all other traits held constant (Magwene 2001). This analysis allows us to determine what traits are significantly dependent on each other (integrated) and to measure the relative strength of that dependence.

To identify the specifics of how two correlation matrices differ, we apply MIBoot (Cole 2002; Cole and Lele 2002; Richtsmeier et al. 2006). Each correlation matrix, one for mouse and one for baboon, are scaled by the mean of their elements and then used to compute a correlation difference matrix by subtracting the elements of one matrix (baboon) from the corresponding elements of the other scaled correlation matrix (mouse). If the correlation matrices are the same (the null hypothesis), the correlation difference is expected to be zero. The bootstrap is used to compute non-parametric confidence intervals ($\alpha \leq 0.10$) for the inter-sample difference in correlations calculated for each linear distance pair within the matrix. To begin, pseudosamples of independent observations are randomly generated using the baboon data and the mouse data. Using the respective pseuodosamples, bootstrap estimates of the sample correlation matrices are scaled for baboon and for mouse and a correlation-difference matrix is estimated. These steps are repeated ≥1,000 times to obtain a bootstrap distribution of correlation difference matrices. The collection of matrices is used to estimate confidence intervals for each of the off-diagonal elements of the matrix. If a confidence interval for a linear distance pair does not include zero (the expected value under the null hypothesis), the null hypothesis of similarity in correlation is rejected for the measurement pair. By testing for similarity for each element of the matrix (each linear distance pair), we can evaluate similarity in magnitude and pattern of correlation, thereby identifying how correlation matrices are similar or different from one another in terms of the anatomy that the correlation coefficients represent.

Genetic Integration—As for the phenotypic estimates, prior to genetic analyses, distance data were regressed on sex and age and the residuals of these regressions were used as our distance data for all genetic estimations. For the baboon sample, pedigree information from SFBR was used with the program Sequential Oligogenic Linkage Analysis Routines (SOLAR) (Almasy and Blangero 1998) to estimate the heritability of the 15 linear distances and to estimate the pairwise genetic correlation between unique pairs of the 15 distances using a polygenic model. From these estimates we constructed a genetic correlation matrix for the 15 pairwise linear distances.

The mouse sample is divided into 83 families and variance components are calculated using a full-sib design following the formula described by Sokal and Rohlf (2000):

$$\sigma^2_{\text{family}} = \frac{MS_{\text{family}} - \sigma^2}{nab}$$

where *nab* represents the number of pups per family. We assume no dominance or epistatic variance and estimate the additive genetic variance for each distance as twice the among-family variance (Ehrich et al. 2005). We estimated heritability as the ratio of the additive genetic variance to the sum of the between-family variance and residual variance (Ehrich et al. 2005). We use Falconer and Mackay's (1996) method to calculate the standard errors. A MANOVA analysis was performed to obtain the between family variance/covariance matrix (G) which was used to obtain the genetic correlation matrix as $R_G = V_A^{-1} G V_A^{-1}$ where V_A^{-1} is the diagonal matrix of additive genetic variances.

All genetic integration comparisons were done for only four of the five developmental modules excluding the incisive alveolar region. In baboons, the heritability estimate for the incisive alveolar distance idp to idi was 0.0 (see below). Therefore, we excluded this distance from the genetic matrices for baboons and mice and limited our comparisons to the four remaining developmental modules and 14 interlandmark distances.

We compared the genetic correlation matrices from the baboon and mouse data with the four theoretical matrices outlining the developmental modules, as well as the theoretical matrix incorporating all four modules using a Mantel's test. These analyses follow the same methods as described for the phenotypic correlation matrices (Cheverud et al. 1989; Cheverud 1995; Marroig and Cheverud 2001). Additionally, we calculated the difference between the average between-module correlation, from the average within-module correlation for the four remaining developmental modules. As with the phenotypic analyses, the permutation results from the Mantel's tests were used to determine if these differences are statistically significant.

We calculated the variance of the eigenvalues of the genetic correlation matrices for the entire mandible as well as for each developmental module using essentially the same method described above for the phenotypic data. As was done in the phenotypic analysis, each observed variance of the eigenvalues was standardized by dividing the observed variance of the eigenvalues by the number of traits minus one (Pavlicev et al. 2009). To correct for the positive bias introduced by small sample sizes we followed the same formula that was used for the phenotypic data described by Cheverud et al. (1989) but used the effective sample size rather than the total number of individuals. The effective sample size is the effective number of independent breeding values represented in the pedigree data (Cheverud 1995, 1996).

We also used conditional independence of the partial genetic correlations. Using Magwene's (2001) method described previously for the phenotypic data, we determined distances that are significantly conditionally dependent (EES) and the strength of the dependence (ES).

Direct Comparisons of Correlation Matrices—We compared the correlation structure between mouse and baboon using Mantel's tests. Comparisons between groups were performed for both phenotypic and genetic correlation matrices using the full matrix of distances (15 for phenotypic, 14 for genetic). Additionally, we compared the phenotypic correlation structure with the genetic correlation structure for both mouse and baboon samples using the 14 distances included in the genetic matrix. Statistical significance was calculated using 1000 permutations. Matrix repeatabilities were calculated for phenotypic and genetic correlation matrices for both baboons and mice. Repeatabilities were calculated by subtracting the average error variance of correlation estimates from the observed variance of correlation estimates divided by the observed variance. These repeatabilities yield an estimate of the maximum correlation that can be expected when two sample matrices are drawn from a common population. Matrix correlations as calculated by Mantel's tests were then standardized by the matrix repeatabilities. For example, the correlation between the

mouse phenotypic correlation matrix and the baboon phenotypic correlation matrix would be corrected using the following formula:

$$Correctedr_{bm}=r_{bm}/\sqrt{t_{baboon} * t_{mouse}}$$

where r_{bm} is the correlation between the baboon and mouse phenotypic correlation matrices and t_{baboon} and t_{mouse} are the repeatabilities for the baboon and mouse phenotypic correlation matrices respectively (Cheverud 1996, pp. 15–16). For comparisons of genetic and phenotypic matrices within each species we must calculate the maximum possible observed correlation as the two matrices are not independent of each other. To calculate the maximum correlation we used the following formula:

$$Maxr_{GOPO}=h^2\sqrt{t_P/t_E}+e^2\sqrt{t_G t_E}-e^2\sqrt{(1-t_G)(1-t_E)(t_P/t_E)}$$

where h^2 is the average heritability for the 14 distances, e^2 is $1 - h^2$; t_P, t_G, and t_E are the repeatabilities for the phenotypic, genetic and environmental correlation matrices, respectively (Cheverud 1996, p. 16). This calculation assumes that heritability is consistent across traits, that the correlation matrices are equal, and that the estimation errors of genetic and environmental correlations are perfectly negatively correlated. Observed matrix correlations between genetic and phenotypic correlation matrices within species are then evaluated relative to these maximum correlations rather than relative to one because the observed similarity of correlation matrices is limited by the estimation error.

Results

Phenotypic Integration

Baboon and mouse phenotypic correlation matrices with associated standard errors can be found in the supplementary materials (Tables S1 and S2) as well as on our website www.hominid.psu.edu. The average correlation in the baboon phenotypic correlation matrix is $r = 0.149$ and $r^2 = 0.059$. Of the 105 individual correlations, 84 are statistically significant at $P \leq 0.05$, although most correlation coefficients are relatively low ($r < 0.5$). There are five linear distance pairs with correlations greater than 0.5 and all are positively correlated and fall within the developmental modules. There are two high correlations within the incisive alveolar region (sms to idi and sms to idp with $r = 0.838$ and sms to idi and sms to mpm with $r = 0.523$), and one within the coronoid process (pcp to iar and mmn to iar with $r = 0.877$), condylar process (pmc to amc and pmc to mmn with $r = 0.785$), and angular process (ang to irb and mac to irb with $r = 0.781$). The average correlation for the mouse phenotypic correlation matrix is $r = 0.134$ and $r^2 = 0.063$. Similar to the baboon matrix, 83 of the 105 individual correlations are statistically significant and most correlations are low ($r < 0.5$). There are eight individual correlations with $r > 0.5$ and as found for baboons, most of these correlations are positive and fall within developmental modules. There are two high correlations within the incisive alveolar region (idp to idi and sms to idp with $r = 0.522$, sms to idi and sms to idp with $r = 0.567$), two within the coronoid process (pcp to iar and pcp to mmn with $r = 0.593$, pcp to iar and mmn to iar with $r = 0.856$), one within the angular process (mac to ang and mac to irb with $r = 0.875$), and one within the condylar process (mmn to amc and pmc to mmn with $r = 0.597$). There are also two high correlations between distances from different developmental modules: a correlation of $r = 0.605$ between a distance from the molar alveolar region and a distance from the incisive alveolar region (mpm to ipm and sms to idp), as well as a negative correlation ($r = -0.566$) between a distance from the molar alveolar region and a distance from the angular process (mpm to iar and mmn to iar).

To determine how well each of the five developmental modules described by Atchley and Hall (1991) fit with the phenotypic correlation structures of the baboon and mouse data, we performed Mantel's tests between the phenotypic correlation matrix of each sample and theoretical matrices. There is a positive and statistically significant correlation between the observed baboon phenotypic correlation matrix and the theoretical matrix that represents the entire mandible (Table 3). The theoretical matrices representing integration of the coronoid process and condylar process are relatively strongly correlated with the observed baboon phenotypic correlations although these correlations fail to reach statistical significance at $P = 0.05$ (Table 3, Fig. 3). Results from our tests for differences in the average between-module correlation and the average within-module correlation for baboons are very similar to the theoretical matrix results (Table 3). The difference between the average correlation within the coronoid process and the average correlation of all other traits is nearly statistically significant (Table 3). Likewise, the difference between the average correlation within the condylar process and the average correlation for the rest of the mandibular traits is nearly significant (Table 3). These results suggest that in baboons the coronoid and condylar processes are highly integrated modules compared with other mandibular components.

The results of the Mantel's test for the mouse data are similar to the results for the baboon correlations. The observed mouse phenotypic correlation matrix is positively and significantly correlated with the theoretical matrix representing the entire mandible and with the theoretical matrix representing the coronoid process which is especially strongly integrated (Table 3, Fig. 3). As with the baboons, our results for the difference between average within-module correlations and average between-module correlations are very similar to our theoretical matrix results. There is a significant difference between the average within-module correlation for the coronoid process and the average correlation between all other traits.

Baboons have significantly greater variance of the eigenvalues than the mice for the condylar process, while mice have significantly greater variance of the eigenvalues relative to baboons for the coronoid process (Fig. 4, Table 4). These results support our findings from the Mantel's tests where mouse data had a much stronger correlation with the coronoid process theoretical matrix, and baboon data were more highly correlated with the condylar process theoretical matrix.

Using partial correlations and the method developed by Magwene (2001) we found the baboon mandible to be most strongly integrated within the angular process followed by the coronoid and condylar processes. In mice, the incisive alveolar module is most strongly integrated followed by the coronoid and condylar processes (Fig. 5). This test does not include a priori expectations of the five developmental modules, but we still find that the most strongly integrated sets of distances fall within the proposed developmental modules.

Elements of the scaled correlation matrices for baboon (Table S1) and mouse (Table S2) are plotted in Fig. 6 along with the elements of the correlation difference matrix estimated by MIboot. As evinced by the correlation matrices for mouse and baboon (Tables S1 and S2), MIBoot results convey a generalized similarity in pattern and magnitude of mandibular integration in mouse and baboon mandibles. Of the 105 elements in the correlation difference matrix, 41 (39%) are shown by confidence interval to be significantly different in the samples compared, but the null hypothesis of similarity in morphological integration cannot be rejected for the remaining 64 linear distance pairs. Of those that are significantly different, 22 linear distance pairs are significantly more strongly correlated in baboon while 19 linear distance pairs are significantly more strongly correlated in mice (Fig. 6). Both samples show a correlation of greater magnitude for at least one linear distance pair within

the condylar, angular and incisive modules, reinforcing our previous findings of strong within module integration for both species (Table 5).

Of the 22 linear distance pairs that are significantly more strongly correlated in baboon, four describe measurement pairs within the condylar, angular, or incisive modules (Fig. 7). The remainder represents between-module relations; most notably the angular and incisive modules show significantly stronger associations with one another in baboon for five linear distance pairs. In addition, elements of the angular and incisive modules each show elevated correlations with elements of the molar alveolar module. Finally the strength of the several correlations between the incisive and the condylar modules and between the angular and the coronoid modules are significantly elevated in baboon. The magnitude of associations within the angular process and between the angular and other modules excepting the condylar process is different from what is observed in mouse (Fig. 7).

Of the 19 linear distance pairs that are significantly more strongly correlated in mice, eight describe measurement pairs within modules (Fig. 7). In a pattern not seen in baboon, the mouse mandible shows significantly stronger patterns of correlation within the coronoid process (Fig. 7). There are eight correlations between the coronoid and incisive alveolar showing significantly stronger association within the mouse mandible. Additionally, there is a pair of measures joining the condylar and coronoid process, the condyle and incisive region, and the condylar and angular modules that show significantly stronger correlation in mouse relative to baboon. Measures of the coronoid process show significantly stronger correlations with linear distances of the condylar, molar alveolar and incisive alveolar modules.

Though these observations generally agree with the results of the previous analyses, the statistical dissection of localized differences in integration patterns reveal between-module associations that are not as apparent when modules are identified a priori. Localized differences in magnitudes of integration reveal associations between the angular process and incisive alveolar region unique to baboons and between the coronoid process and the incisive alveolar region unique to mice. These species specific differences in magnitudes of association must be considered against an overall similarity in mandibular morphological integration patterns in the two species (Fig. 6).

Genetic Integration

Heritability estimates, their standard errors and probabilities of the null model were calculated for all 15 traits in the baboon and mouse samples. The average h^2 for the distances in the baboon sample is 0.26, ranging from 0 to 0.57 (Table 6). An adequate effective sample size, which is the number of independent breeding values represented in the pedigree data, is necessary to ensure that genetic correlations can be accurately estimated (Cheverud 1995, 1996). The incisive alveolar distance idp to idi for the baboon sample had a h^2 estimate of 0.0 (Table 6) resulting in an effective sample size for this distance that was too low to be included in further genetic analyses. Therefore, we removed the distance idp to idi from our matrices and the incisive alveolar module from our analyses of genetic data for both mice and baboons. All distances in the mouse sample had significant h^2 estimates at $P \leq 0.05$ (Table 6). The average mouse h^2 for mandibular distances is 0.41 with a range of 0.12 to 0.64.

Genetic correlation matrices and their associated standard errors for both baboon and mouse data can be found in the supplementary materials (Tables S3 and S4) as well as on our website (www.hominid.psu.edu). The average correlation for the baboon genetic correlation matrix is $r = 0.114$ and $r^2 = 0.177$. Of the 105 correlations, there are 18 with $r > 0.5$ and 14 correlations that are statistically significant at $P \leq 0.05$. Unlike the baboon phenotypic

correlation matrix, many of the strongest correlations are negative and are between distances located in different developmental modules. Highly negative correlations are found between distances from the molar alveolar region and the coronoid process (mpm to ipm and pcp to iar with $r = -0.866$, mpm to ipm and mmn to iar with $r = -0.881$), between distances from the coronoid and condylar processes (mmn to amc and pcp to iar with $r = -0.943$, and mmn to amc and mmn to iar with $r = -0.81$), and between the molar alveolar region and the angular process (ang to irb and mpm to ipm with $r = -0.71$). These specific results are obtained by restricting the parameter space to a −0.90 to 0.90 interval as they otherwise move to the boundary and the information matrix cannot be inverted. This raises concern over the accuracy of these specific values and their standard errors and, given the relatively small sample size, it may be advisable to disregard these high negative values when interpreting our results. It is also possible that these highly negative correlations could be a function of hybridity in the baboon sample. To check for this possibility, we re-calculated the genetic correlations that were highly negative using only pure-bred anubis baboons. Our results did not change substantially, and it is difficult to determine whether the changes that did occur were due to a reduced sample size or due to hybridity.

The mouse genetic correlation matrix is different from the estimated baboon matrix and more closely resembles the phenotypic matrices having no high negative correlations. There are 53 statistically significant individual correlations with 17 correlations with $r > 0.5$, all of which are positive. The average correlation is $r = 0.214$ and $r^2 = 0.132$. As with the baboon genetic matrix, many of these relatively high correlations are for distances occupying different developmental modules, although the highest correlations ($r \geq 0.7$) represent linear distances pairs that reside within developmental modules. These strong positive correlations include one within the incisive alveolar region (sms to idi and sms to idp with $r = 0.862$), two within the coronoid process (pcp to iar and mmn to iar with $r = 0.870$, pcp to iar and pcp to mmn with $r = 0.713$), one within the condylar process (mmn to amc and pmc to mmn with $r = 0.742$) and one within the angular process (mac to ang and mac to irb with $r = 0.834$).

The results of our Mantel's tests indicate that the theoretical matrix representing all four remaining modules is significantly correlated with the observed genetic correlation matrices for both baboon and mouse (Table 7). The theoretical matrix representing strong integration within the condylar process was nearly statistically significantly correlated with the baboon genetic correlation matrix (Fig. 8, Table 7). The mouse genetic correlation matrix was positively and significantly correlated with the coronoid theoretical matrix (Fig. 8, Table 7). These results are similar to our results using phenotypic correlation matrices and suggest that the pattern of integration includes relationships among all of the different modules. Our results for the differences between the average within-module correlations and average between-module correlations for the four developmental modules tested are similar to our results from Mantel's tests. These results suggest that the baboon genetic data are most tightly integrated within the condylar process, whereas mouse genetic data are most highly integrated within the coronoid process (Table 7).

Our analysis using variance of the eigenvalues to compare the strength of integration between mice and baboons indicates that mice are equally or more strongly integrated than baboons for the entire mandible as well as all developmental modules except the condylar process (Table 8). We are unable to test if these differences are significant because the effective sample size for baboons is too small, and the genetic correlation matrix is too ill-conditioned to perform permutation tests. Our observed results do account for differences in sample size, and therefore, it is likely that the variance of eigenvalues reported for the baboon sample are underestimated. Thus, it is of interest that the baboons show greater

integration within the condylar process as compared with mice even with the large baboon correction factor.

Magwene's (2001) conditional independence test reveals that patterns of genetic integration are quite different in our baboon and mouse samples. In baboons, there are no significant partial correlations, perhaps as a result of sample size restrictions. However, for our mouse sample there are several strong partial correlations, each of which falls within a developmental module. Very strong partial correlations for distances within the coronoid process and within the condylar process were found for mice and additional strong partial correlations in mice were found for distances within the angular process and within the molar alveolar region.

Direct Comparisons of Correlation Matrices

Our comparison of phenotypic matrices between mouse and baboon using Mantel's test suggest that both species have a very similar correlation structure. After correcting for repeatabilities the correlation between the two phenotypic matrices is over 1.0, indicating a very tight matrix correlation between mouse and baboon phenotypic relationships. The correlation between the genetic correlation matrices between the two species is not especially high, even after correction for repeatabilities, with $r = 0.39$. However, this result is nearly entirely driven by the aberrant low negative genetic correlations in the baboon matrix. If those negative correlations that greatly influence the observed variance of correlation values across the matrix are removed, the apparent repeatability of the baboon genetic correlation matrix is decreased and the relative correlation between the mouse and baboon genetic correlation matrices increases from 0.39 to 0.87. Before correction, the correlation between the baboon phenotypic and genetic correlation matrices is 0.49. However, the maximum correlation that can be obtained for these two matrices is 0.52, reducing the maximum correlation to 0.94 instead of a perfect correlation of 1.0. For mice, the correlation between the genetic and phenotypic correlation matrices before correction is 0.84, with a maximum correlation of 0.87 which reduces the maximum correlation possible from 1.0 to 0.96. After correction for matrix repeatabilities, correlations between genetic and phenotypic correlation structures are quite high for both species with $r = 0.89$ for baboons and $r = 0.90$ for mice. Therefore, the correlations between phenotypic and genetic correlation matrices for both baboons and mice are as similar as can be expected if the true population values are nearly identical. These results indicate that the correlation structures and therefore, integration patterns, are very similar for mouse and baboon phenotypic data. They also suggest that both mouse and baboon phenotypic correlation data closely represent their genetic correlation data.

Discussion

To better understand the development and evolution of complex structures, we often look for broad trends across a wide range of species and then begin to pinpoint the specific processes that create differences between species. The developmental pathways involved in craniofacial development are thought to be generally similar across mammalian species (Langille and Hall 1989; Trainor and Krumlauf 2001; Wilkins 2002; Hallgrímsson et al. 2004). These hypothesized and observed similarities are the basis for our use of model organisms—such as the mouse—to inform us of the mechanisms underlying cranial development in studying human disease and normal variation. Our study compares patterns of mandibular morphological integration between baboons and mice to determine if the mandibles of both species display similar patterns of developmental modularity.

Overall, there is a striking similarity in the correlation patterns for baboons and mice for both phenotypic and genetic data. Specifically, both the phenotypic and genetic correlation

structures for baboons and mice generally follow the modular pattern of integration suggested by Atchley and Hall (1991). Structures within the coronoid, condylar, and alveolar processes, as well as structures within the incisive and molar alveolar regions are generally highly correlated with each other. This pattern of integration was borne out using both a priori and a posteriori tests. This similarity of mandibular integration patterns is in keeping with several studies that have compared cranial integration between different primate species. Cheverud (1996) compared phenotypic, genetic and environmental correlation matrices between cotton-top and saddle-back tamarins and found that patterns of correlation were similar between species. Ackermann and Cheverud (2000) expanded this study to a comparison of cranial integration in six species of tamarins and again found that patterns of integration were similar across all species. In a comprehensive study that compared 40 species of New World monkeys, Marroig and Cheverud (2001) found that in general, all species showed a similar pattern of cranial integration with the oral region showing the strongest integration. This pattern of strong integration of the oral region has also been found for adult apes and humans (González-José et al. 2004; Ackermann 2005; Mitteroeker and Bookstein 2008). In fact, cranial integration has been found to be widely similar across therian mammals with strong within-module integration of the oral-nasal region and the anterior cranial base (Goswami 2006).

While our results confirm our hypothesis of similar integration patterns, the extent of similarity between these two species is somewhat surprising given the marked structural and functional differences between mouse and baboon mandibles. Mice have very large, ever-growing incisors with roots that extend throughout most of the body of the mandible. The forces applied to the exposed aspect of the incisor are received along the root influencing bone growth along the body of the mandible. Mice also have a large diastema between incisor and molar teeth that is absent in baboons, the space being populated by an additional incisor, canine and premolar teeth. Baboons, particularly males, have extremely large canines that in addition to mastication are used in defense as well as sexual display. In addition, the mouse mandibular symphysis remains unfused in life while the baboon mandibular symphysis fuses prenatally or soon after birth. Mice tend to move their mandibles from front to back when using their molars to chew, whereas baboon molar chewing involves a side to side motion. The medial-lateral mandibular motion used by baboons to chew requires a much larger ratio of balancing-side to working-side force than is required of anterior-posterior chewing in the mouse (Weijs and deJongh 1977; Beecher 1979, Hylander 1979a, b). The difference in chewing strategy requires differences in bone mass, muscle morphology, and in the coordination of the muscles of mastication which leads to a different combination of forces exerted on the mandible during mastication. It seems likely that these structural and functional differences overlay the common effects of similar development creating the few differences in integration patterns found between the two species.

The baboon sample appears to have greater cohesion within the condylar process as compared to mice, while mouse mandibles are more strongly integrated within the coronoid process and incisive alveolar module. These specific patterns of integration seem to correspond with the different modes of mastication between the species. The medial-lateral chewing of baboons places stress on the condylar process, potentially increasing integration within that region. Likewise, the anterior-posterior chewing pattern in mice, and the relatively large role their incisors play during mastication likely creates the strong integration within the coronoid process and incisive alveolar region observed. Phenotypic results from Magwene's method using partial correlations revealed further differences between species. Baboon mandibles were found to be strongly correlated within the condylar and coronoid processes but were most strongly correlated within the angular process. Mice were found to be most strongly integrated within the incisive alveolar region

followed by the coronoid process. Partial correlations remove the effects of common variables. It is possible that partial correlations uncover specific functional differences between the species that are obscured in our other analyses that include the effects of common variables such as size and the functional requirements of the mandible as a whole.

Another finding of our study is that patterns of phenotypic and genetic integration are very similar for both mice and baboons. These results suggest that functional and developmental factors acting at the individual level and that influence patterns of phenotypic integration have a heritable basis in both species. Additionally, if the extremely high negative correlations found in the baboon genetic correlation matrix are disregarded, there is a high correlation between mouse and baboon genetic correlation matrices. These results suggest that the heritable basis of the developmental factors responsible for the phenotypic integration pattern is similar for mice and baboons, and therefore, patterns of mandibular integration for both species should respond similarly to most evolutionary forces including selection and drift.

Our results reflect Cheverud's (1996) suggestion that developmental and functional factors are dynamically linked and their interactions create the patterns of integration found in adult morphology. The modular pattern of integration found in both species underlies the ability for structurally different mandibles to have such similar patterns of correlation and potential response to selection. Overall, integration patterns are the same between these two species, possibly reflecting common development and the importance of coordinated mandibular function for mastication. However, having these tightly integrated modules nested within the mandible as a whole, gives the different mandibular components that comprise these modules some autonomy, and therefore, freedom to vary. The partial dissociation among modules, both phenotypically and genetically, are likely due to differing functional demands and may have led to the large structural differences found between the two species, while maintaining the functional integrity of the mandible as a whole. While the two samples studied here support this evolutionary scenario, far more evidence from different species is required to fully address this hypothesis.

Supplementary Material

Refer to Web version on PubMed Central for supplementary material.

Acknowledgments

We thank everyone who participated in the Morphological Integration symposium at the American Association of Physical Anthropology meetings in Columbus, Ohio for their stimulating discussions on integration which have greatly influenced this manuscript. We are grateful to Ryan Adams for technical assistance. We also thank all of the members of the Genomics of Cranial Morphology Consortium especially Alan Walker and Ken Weiss for their insightful comments and suggestions that greatly improved this study. Funding for this study was provided by NSF grants BCS 0522112, BCS 0523305, BCS 0523637, BCS 0725031, BCS 0725068, and BCS 0725227.

References

Ackermann RR. Ontogenetic integration of the hominoid face. Journal of Human Evolution. 2005; 48:175–197.10.1016/j.jhevol.2004.11.001 [PubMed: 15701530]

Ackermann RR, Cheverud JM. Phenotypic covariance structure in tamarins (genus: *Saguinus*): A comparison of variation patterns using matrix correlation and common principal component analysis. American Journal of Physical Anthropology. 2000; 111:489–501.10.1002/(SICI)1096-8644(200004)111:4<489::AI D-AJPA5>3.0.CO;2-U [PubMed: 10727968]

Almasy L, Blangero J. Multipoint quantitative-trait linkage analysis in general pedigrees. American Journal of Human Genetics. 1998; 62:1198–1211.10.1086/301844 [PubMed: 9545414]

Atchley WR, Hall BK. A model for development and evolution of complex morphological structures. Biological Reviews of the Cambridge Philosophical Society. 1991; 66:101–157.10.1111/j.1469-185X.1991.tb01138.x [PubMed: 1863686]

Atchley WR, Plummer AA, Riska B. Genetics of mandible form in the mouse. Genetics. 1985; 111:555–577. [PubMed: 4054609]

Beecher RM. Functional significance of mandibular symphysis. Journal of Morphology. 1979; 159:117–130.10.1002/jmor.1051590109 [PubMed: 423251]

Berg RL. The ecological significance of correlational pleiades. Evolution; International Journal of Organic Evolution. 1960; 14:171–180.10.2307/2405824

Cheverud JM. Phenotypic, genetic, and environmental morphological integration in the cranium. Evolution; International Journal of Organic Evolution. 1982; 36:499–516.10.2307/2408096

Cheverud JM. A comparative analysis of morphological variation patterns in the papionins. Evolution; International Journal of Organic Evolution. 1989; 43:1737–1747.10.2307/2409389

Cheverud JM. Morphological integration in the saddle-back tamarin (*Saguinus fuscicollis*) cranium. American Naturalist. 1995; 145:63–89.10.1086/285728

Cheverud JM. Quantitative genetic analysis of cranial morphology in the cotton-top (*Saguinus oedipus*) and saddleback (*S. fuscicollis*) tamarins. Journal of Evolutionary Biology. 1996; 9:5–42.10.1046/j.1420-9101.1996.9010005.x

Cheverud, JM. Modular pleiotropic effects of quantitative trait loci on morphological traits. In: Schlosser, G.; Wagner, GP., editors. Modularity in development and evolution. Chicago: University of Chicago Press; 2004. p. 132-153.

Cheverud JM, Hartman SE, Richtsmeier JT, Atchley WR. A quantitative genetic analysis of localized morphology in mandibles of inbred mice using finite element scaling. Journal of Craniofacial Genetics and Developmental Biology. 1991; 11:122–137. [PubMed: 1761645]

Cheverud JM, Routman EJ, Irschick DJ. Pleiotropic effects of individual gene loci on mandibular morphology. Evolution; International Journal of Organic Evolution. 1997; 51:2006–2016.10.2307/2411021

Cheverud JM, Wagner GP, Dow MM. Methods for the comparative analysis of variation patterns. Systematic Zoology. 1989; 38:201–213.10.2307/2992282

Cole, TM, III. MIBoot: Software for bootstrap comparison of morphological integration patterns. Kansas City: University of Missouri—Kansas City School of Medicine; 2002.

Cole TM III, Lele S. Bootstrap-based methods for comparing morphological integration patterns. American Journal of Physical Anthropology. 2002; (Supplement 34):55. (Abstract).

Council, NR. Guide for the care and use of laboratory animals. Washington, DC: National Academy of Sciences; 1996.

Darvasi A, Soller M. Advanced intercross lines, an experimental population for fine genetic mapping. Genetics. 1995; 141:1199–1207. [PubMed: 8582624]

Ehrich TH, Kenney-Hunt J, Pletscher S, Cheverud JM. Genetic variation and correlation of dietary response in an advanced intercross mouse line produced from two divergent growth lines. Genetical Research Cambridge. 2005; 85:211–222.

Ehrich TH, Vaughn TT, Koreishi SF, Linsey RB, Pletscher LS, Cheverud JM. Pleiotropic effects on mandibular morphology I. Developmental morphological integration and differential dominance. The Journal of Experimental Zoology. 2003; 296B:58–79. (Molecular and Developmental Evolution). 10.1002/jez.b.9

Falconer, DS.; Mackay, TFC. Introduction to quantitative genetics. 4. London, UK: Pearson Prentice Hall; 1996.

Gass, GL.; Bolker, JA. Modularity. In: Olson, W., editor. Keywords and concepts in evolutionary developmental biology. Cambridge: Harvard University Press; 2002.

González-José R, Van Der Molen S, González-Pérez S, Hernández M. Patterns of phenotypic covariation and correlation in modern humans as viewed from morphological integration. American Journal of Physical Anthropology. 2004; 123:69–77.10.1002/ajpa.10302 [PubMed: 14669238]

Goodale H. A study of the inheritance of body weight in the albino mouse by selection. The Journal of Heredity. 1938; 29:101–112.

Goodale H. Progress report on possibilities in progeny test breeding. Science. 1941; 94:442–443.10.1126/science.94.2445.442 [PubMed: 17758319]

Goswami A. Cranial modularity shifts during mammalian evolution. American Naturalist. 2006; 168:270–280.10.1086/505758

Hallgrímsson B, Willmore K, Dorval C, Cooper DML. Craniofacial variability and modularity in macaques and mice. The Journal of Experimental Zoology. 2004; 302B:207–225. Molecular and Developmental Evolution. 10.1002/jez.b.21002

Hylander WL. Mandibular function in *Galago crassicaudatus* and *Macaca fascicularis*: An in vivo approach to stress analysis of the mandible. Journal of Morphology. 1979a; 159:253–296.10.1002/jmor.1051590208 [PubMed: 105147]

Hylander WL. The functional significance of primate mandibular form. Journal of Morphology. 1979b; 160:223–240.10.1002/jmor.1051600208 [PubMed: 458862]

Klingenberg CP, Leamy LJ, Cheverud JM. Integration and modularity of quantitative trait locus effects on geometric shape in the mouse mandible. Genetics. 2004; 166:1909–1921.10.1534/genetics.166.4.1909 [PubMed: 15126408]

Klingenberg CP, Mebus K, Auffray JC. Developmental integration in a complex morphological structure: How distinct are the modules in the mouse mandible. Evolution & Development. 2003; 5:522–531.10.1046/j.1525-142X.2003.03057.x [PubMed: 12950630]

Langille RM, Hall BK. Developmental processes, developmental sequences and early vertebrate phylogeny. Biological Reviews of the Cambridge Philosophical Society. 1989; 64:73–91.10.1111/j.1469-185X.1989.tb00672.x [PubMed: 2675995]

Leamy LJ. Morphological integration of fluctuating asymmetry in the mouse mandible. Genetica. 1993; 89:139–153.10.1007/BF02424510

Lessells CM, Boag PT. Unrepeatable repeatabilities: A common mistake. The Auk. 1987; 104:116–121.

MacArthur J. Genetics of body size and related characters. I. Selection of small and large races of the laboratory mouse. American Naturalist. 1944; 78:142–157.10.1086/281181

Magwene PM. New tools for studying integration and modularity. Evolution; International Journal of Organic Evolution. 2001; 55:1734–1745.

Marroig G, Cheverud JM. A comparison of phenotypic variation and covariation patterns and the role of phylogeny, ecology, and ontogeny during cranial evolution of new world monkeys. Evolution; International Journal of Organic Evolution. 2001; 55:2576–2600.

Mezey JG, Cheverud JM, Wagner GP. Is the genotype-phenotype map modular? A statistical approach using mouse quantitative trait loci data. Genetics. 2000; 156:305–311. [PubMed: 10978294]

Mitteroeker P, Bookstein F. The evolutionary role of modularity and integration in the hominoid cranium. Evolution; International Journal of Organic Evolution. 2008; 62:943–958.10.1111/j.1558-5646.2008.00321.x

Needham J. On the dissociability of the fundamental processes in ontogenesis. Biological Reviews of the Cambridge Philosophical Society. 1933; 8:180–223.10.1111/j.1469-185X.1933.tb01153.x

Norgard EA, Roseman CC, Fawcett GL, Pavlicev M, Morgan CD, Pletscher LS, et al. Identification of quantitative trait loci affecting murine long bone length in a two-generation intercross of LG/J and SM/J mice. Journal of Bone and Mineral Research. 2008; 23:887–895.10.1359/jbmr.080210 [PubMed: 18435578]

Olson, EC.; Miller, RL. Morphological integration. Chicago: University of Chicago Press; 1958.

Pavlicev M, Cheverud JM, Wagner GP. Measuring morphological integration using eigenvalue variance. Evolutionary Biology. 2009 in press.

Ramaesh T, Bard JBL. The growth and morphogenesis of the early mouse mandible: A quantitative analysis. Journal of Anatomy. 2003; 203:213–222.10.1046/j.1469-7580.2003.00210.x [PubMed: 12924821]

Richtsmeier JT, Aldridge KA, DeLeon VB, Panchal J, Kane AA, Marsh JL, et al. Phenotypic integration of neurocranium and brain. Journal of Experimental Zoology (Molecular and Developmental Evolution). 2006; 306B:1–19.

Schlosser, G.; Wagner, GP. Introduction: The modularity concept in developmental and evolutionary biology. In: Schlosser, G.; Wagner, GP., editors. Modularity in development and evolution. Chicago: University of Chicago Press; 2004. p. 1-11.

Simon HA. The architecture of complexity. Proceedings of the American Philosophical Society. 1962; 106:467–482.

Sokal, RS.; Rohlf, FJ. Biometry. New York: H.W. Freeman; 2000.

Trainor PA, Krumlauf R. Hox genes, neural crest cells and brachial arch patterning. Current Opinion in Cell Biology. 2001; 13:698–705.10.1016/S0955-0674(00)00273-8 [PubMed: 11698185]

Valeri CJ, Cole TM III, Lele S, Richtsmeier JT. Capturing data from three-dimensional surfaces using fuzzy landmarks. American Journal of Physical Anthropology. 1998; 107:113–124.10.1002/(SICI)1096-8644(199809)107:1<113::AID-AJPA9>3.0.CO;2-O [PubMed: 9740305]

Wagner GP. On the eigenvalue distribution of genetic and phenotypic dispersion matrices: Evidence for a nonrandom organization of quantitative character variation. Journal of Mathematical Biology. 1984; 21:77–95.

Wagner GP. A comparative study of morphological integration in Apis mellifera (Insecta, Hymenoptera). Journal of Zoological Systematics and Evolutionary Research. 1990; 28:48–61.

Wagner GP. Homologues, natural kinds and the evolution of modularity. American Zoologist. 1996; 36:36–43.

Washburn SL. The relation of the temporal muscle to the form of the skull. The Anatomical Record. 1947; 99:239–248.10.1002/ar.1090990303 [PubMed: 20270605]

Weijs WA, deJongh HJ. Strain in mandibular alveolar bone during mastication in the rabbit. Archives of Oral Biology. 1977; 22:667–675.10.1016/0003-9969(77)90096-6 [PubMed: 272139]

Wilkins, AS. The evolution of developmental pathways. Sunderlan, MA: Sinauer; 2002.

Willmore KE, Young NM, Richtsmeier JT. Phenotypic variability: Its components, measurement and underlying developmental processes. Evolutionary Biology. 2007; 34:99–120.10.1007/s11692-007-9008-1

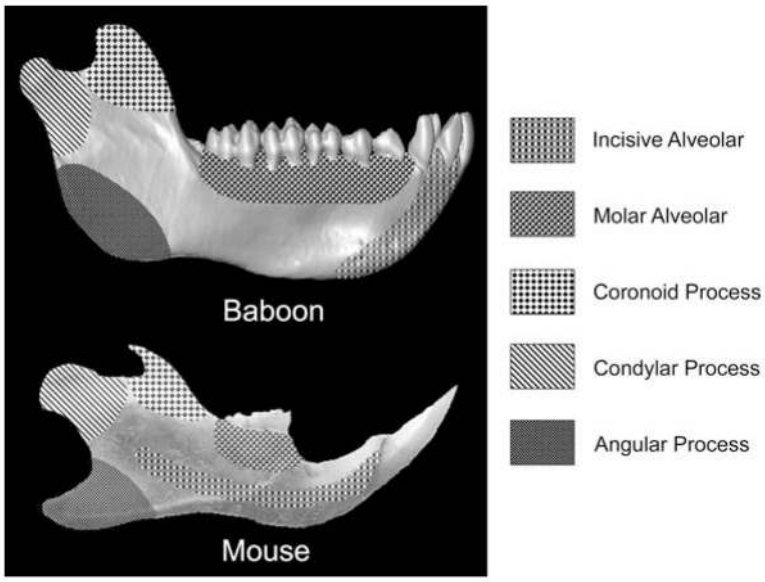

Fig. 1.
Illustration of the five mandibular developmental modules used for this study as outlined by Atchley and Hall (1991). The five modules are shown on a lateral view of the baboon mandible (*above*) and mouse mandible (*below*)

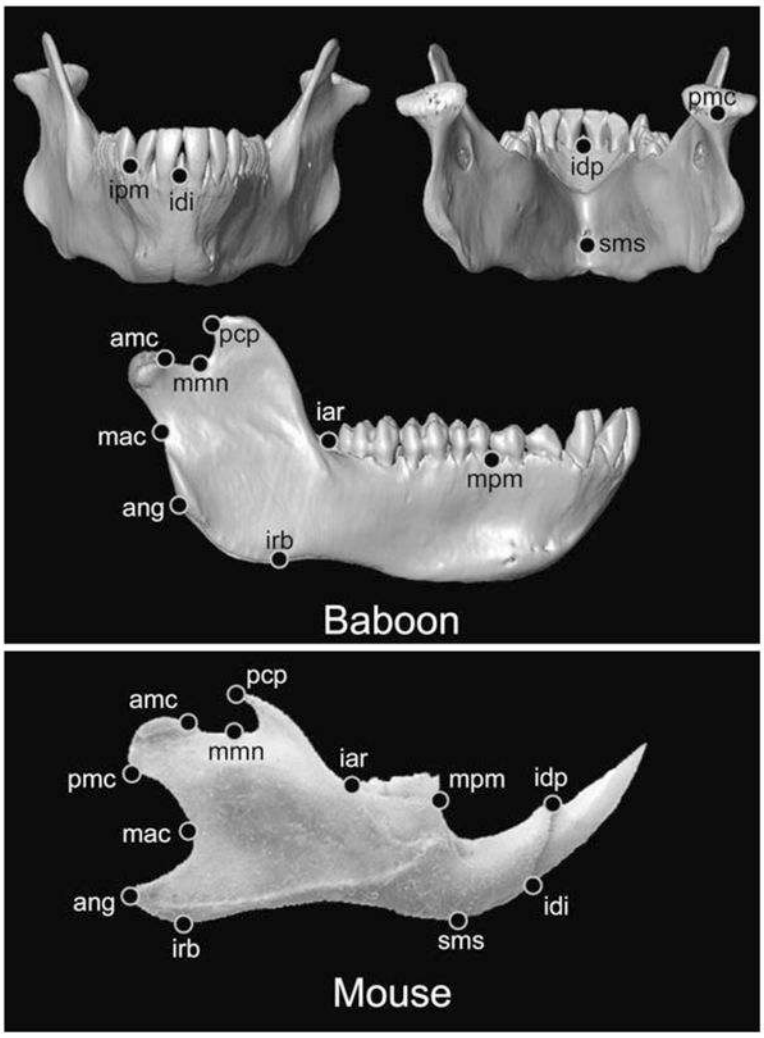

Fig. 2.

Homologous landmarks taken from both baboon and mouse mandibles. Baboon data include 13 three-dimensional landmarks digitized from medical CT images. Mouse data were collected from digital photographs and include 12 two-dimensional landmarks from the right hemi-mandible. Baboon mandibles are depicted in anterior view (*top left*), posterior view (*top right*), and right lateral (bottom). The mouse mandible is shown in right lateral view

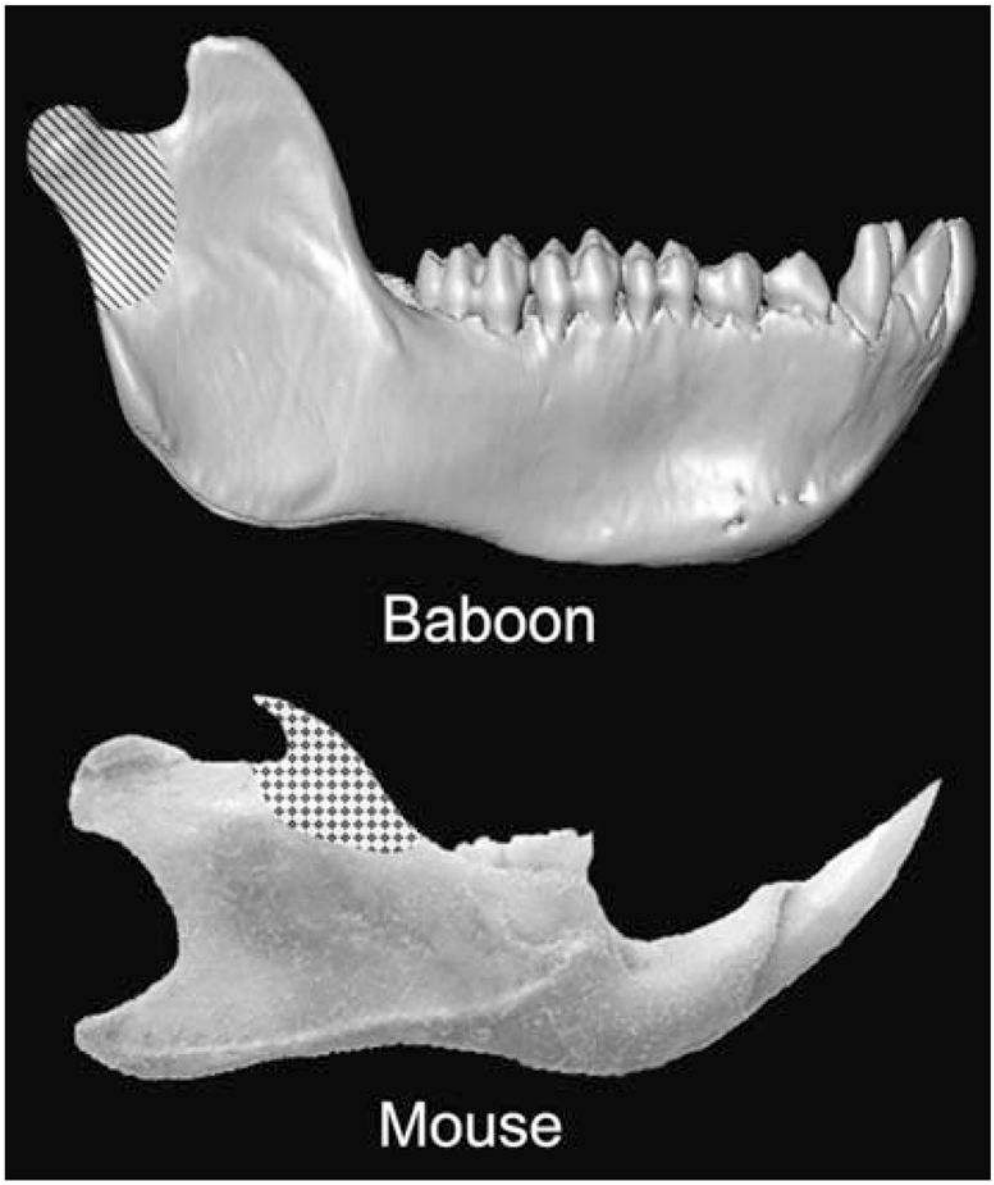

Fig. 3.

Results from matrix correlations using Mantel's tests between the observed phenotypic correlation matrices for the baboon and mouse samples and the five theoretical correlation matrices that depict the developmental modules of Atchley and Hall (1991). Both groups are significantly integrated among the five modules (*not shown*), mice (*below*) are significantly integrated within the coronoid process, and baboons (*above*) are nearly significantly integrated within the condylar process

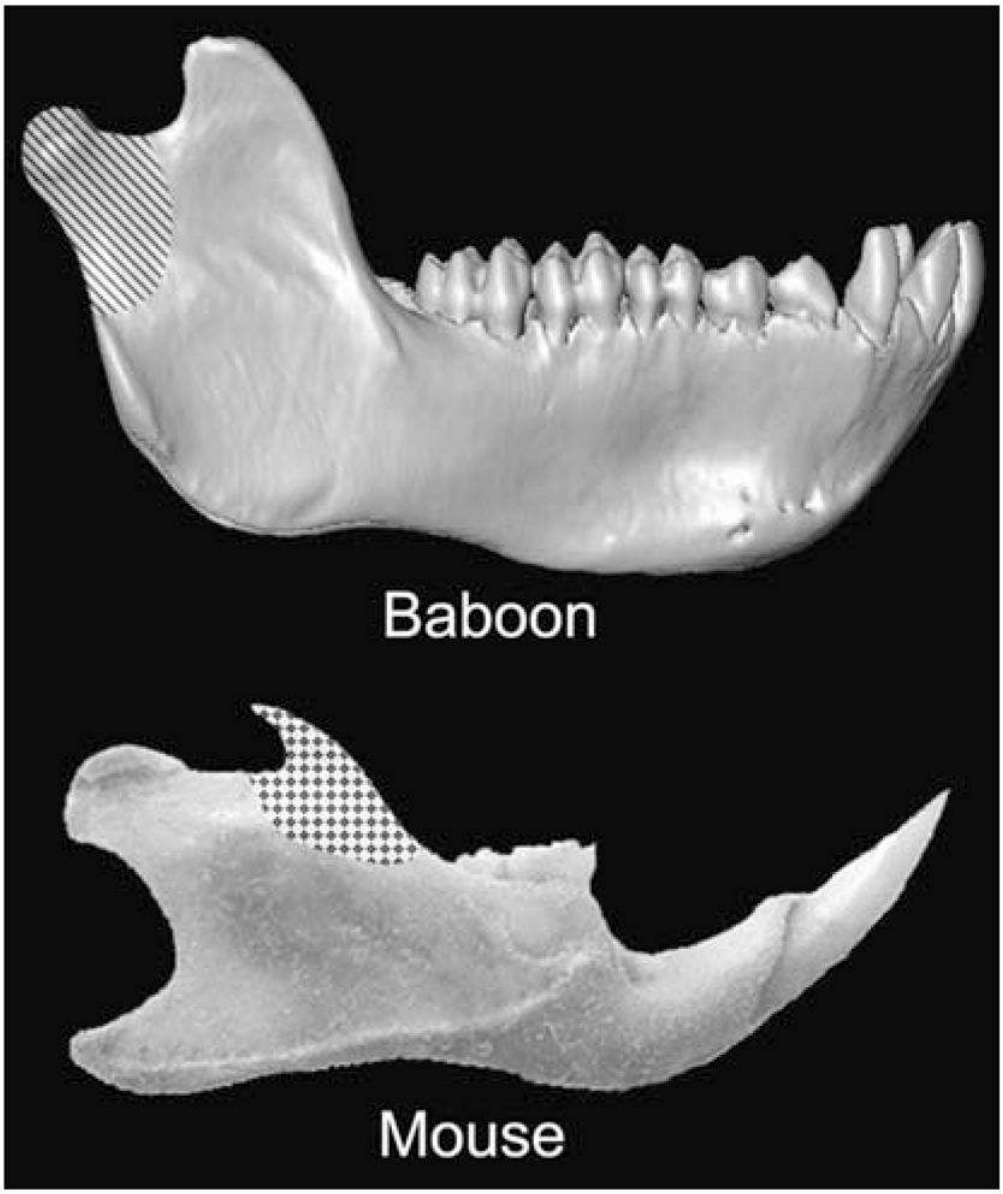

Fig. 4.

Results from Wagner's (1991) variance of the eigenvalues analysis for phenotypic correlation data. Baboons have significantly greater variance of the eigenvalues than mice for the condylar process. Mice have significantly larger variance of the eigenvalues than baboons for the coronoid process

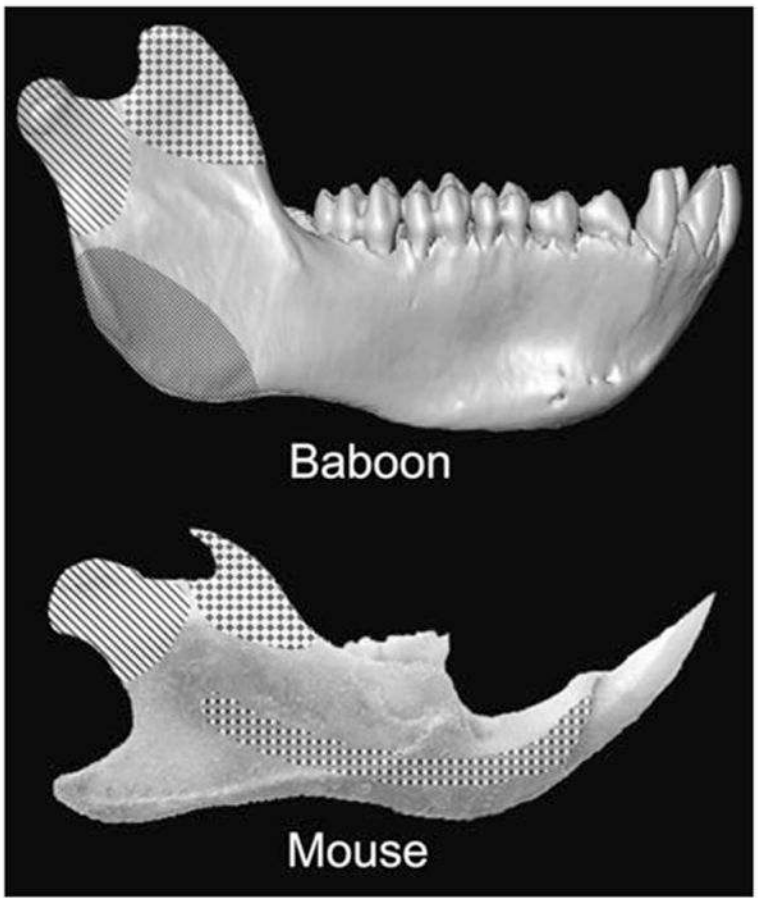

Fig. 5.

Results from Magwene's (2001) partial correlation analysis of the phenotypic data. Distances within the angular, coronoid and condylar processes are conditionally dependent in baboons. Mouse phenotypic data also show conditional dependence within the coronoid process and condylar process, as well as within the incisive alveolar region

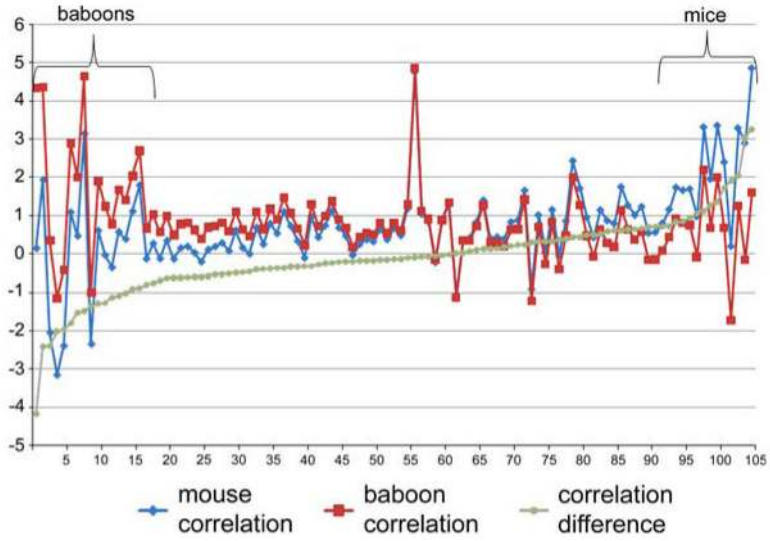

Fig. 6.

Graph of scaled correlation coefficients between linear distance pairs for mouse (*dark grey diamonds*) and baboon (*black squares*) and correlation differences (*light grey circles*) between mouse and baboon. Estimates of the scaled correlation coefficients for each linear distance pair and for correlation differences are given on the y-axis. Linear distance pairs are listed on the x-axis sorted by correlation difference values. The ordered list of the specific distance pairs plotted along the x-axis is given in Table S5. Note the generalized similarity in correlation values in both mouse and baboon. Brackets on the far left and far right of the graph indicate the sets of linear distance pairs with correlation values that are significantly different between mouse and baboon by confidence interval ($\alpha = 0.10$)

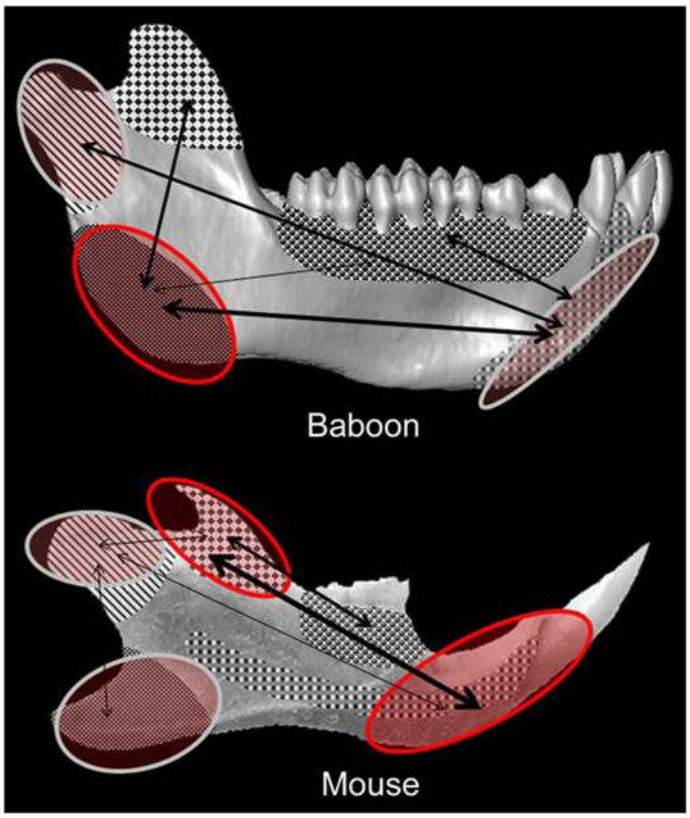

Fig. 7.

Linear distance pairs that show significantly stronger magnitudes of association in baboon (*top*) and mouse (*bottom*) as revealed by MIBoot. On each mandible, modules that are circled and shaded in red have at least one linear distance pair within the module that has a significantly stronger correlation relative to the other species. Those modules in which the red circle is outline in red have more than one within-module linear distance pair that is significantly more strongly correlated in that species. Arrows between modules indicate between-module linear distance pairs that are significantly stronger in one species. The thickness of the arrows indicates the relative number of linear distance pairs showing significantly different correlation magnitudes for any particular inter-module correlation

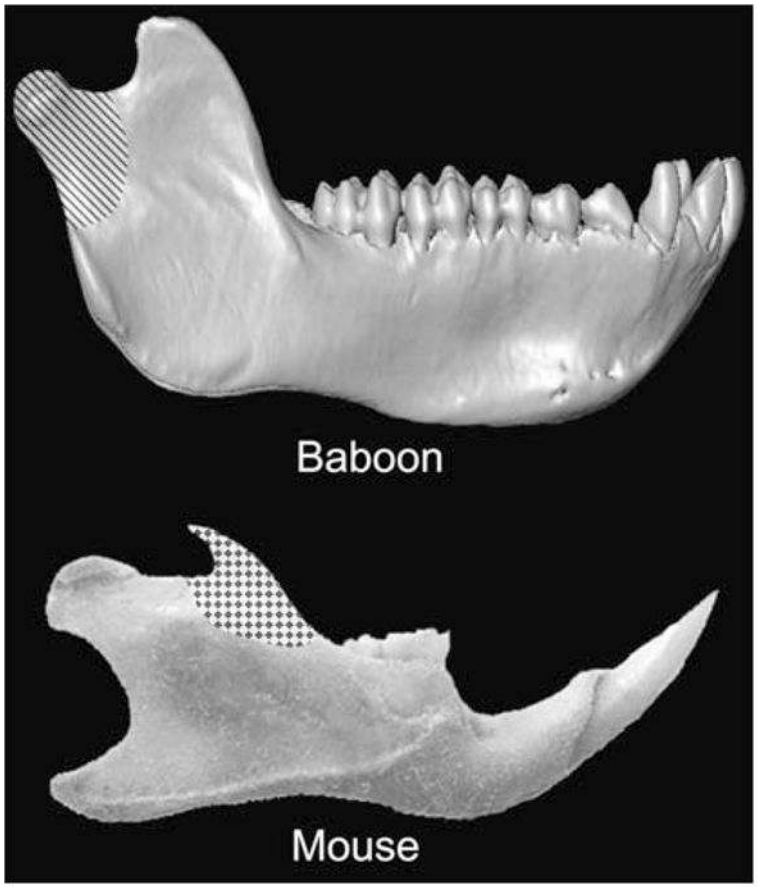

Fig. 8.

Matrix correlation results using Mantel's tests between observed genetic correlation matrices and theoretical matrices for baboons (*above*) and mice (*below*). The observed genetic correlation matrices of both groups are significantly correlated with the theoretical matrix that represents all four modules (*not shown*). The baboon genetic correlation matrix is also significantly correlated with the condylar theoretical matrix, and the mouse genetic correlation matrix is significantly correlated with the coronoid process theoretical matrix

Table 1

List of landmarks used in this study and their anatomical descriptions

Landmark	Anatomical description
idp	Infradentale posterior—mandibular
idi	Infradentale inferior
sms	Superior mental spine
mpm	Molar-premolar junction at lateral alveolar border of mandible
iar	Mandibular tuberosity
ipm	Premaxilla-maxilla junction at lateral alveolar border of mandible (baboon only)
pcp	Posterior portion of coronoid process—superiormost point on posterior edge
mmn	Mid-mandibular notch—deepest point of curvature
pmc	Posterior mandibular condyle
amc	Anterior mandibular condyle
mac	Midpoint along posterior ramus between mandibular angle and condylar process
ang	Mandibular angle—posterior aspect
irb	Inferior border between ramus and body of mandible

Mouse landmarks are 2D whereas baboon landmarks are 3D

Table 2

15 interlandmark distances calculated from 2D landmarks (mice) and 3D landmarks (baboons)

Distance	Developmental module
idp to idi	Incisive alveolar
sms to idi	Incisive alveolar
sms to idp	Incisive alveolar
mpm to iar	Molar alveolar
mpm to ipm	Molar alveolar (Baboon)
mpm to idp	Molar alveolar (Mouse)
sms to mpm	Molar alveolar
pcp to iar	Coronoid process
pcp to mmn	Coronoid process
mmn to iar	Coronoid process
pmc to amc	Condylar process
mmn to amc	Condylar process
pmc to mmn	Condylar process
mac to ang	Angular process
ang to irb	Angular process
mac to irb	Angular process

Table 3

Results from Mantel's tests between phenotypic correlation matrices of mouse and baboon data with hypothetical matrices for five developmental modules, as well as the average within-module correlation and between-module correlation with significance values for their differences

Developmental module	Baboon				Mouse			
	Mandible *r*	Within-module *r*	Between-module *r*	*P* Value	Mandible *r*	Within-module *r*	Between-module *r*	*P* value
All modules	**0.303**	**0.292**	**0.130**	**0.001**	**0.286**	**0.283**	**0.110**	**0.005**
Incisive	0.126	0.291	0.149	0.226	0.086	0.241	0.131	0.391
Molar	0.020	0.174	0.152	0.851	0.018	0.156	0.134	0.454
Coronoid	**0.201**	**0.373**	**0.146**	**0.059**	**0.321**	**0.531**	**0.123**	**0.002**
Condylar	**0.197**	**0.369**	**0.147**	**0.074**	0.031	0.173	0.133	0.759
Angular	0.092	0.254	0.150	0.340	0.145	0.313	0.129	0.195

The between-module correlation represents the average correlation of all distances that are not within the module of interest. For instance for the coronoid module, the within-module correlation is the average correlation for all distance correlations within the coronoid process and the between-module correlation is the average correlation of all other distance correlations. Significant or nearly significant correlations and differences in correlations at the $P = 0.05$ level are highlighted in bold

Table 4

Comparison of the variance of the eigenvalues for baboon and mouse phenotypic correlation matrices for the entire mandible and the five developmental modules and their associated *P* values

Developmental module	Baboon	Mouse	*P* Value
Whole mandible	0.061	0.067	0.277
Incisive	0.351	0.364	0.436
Molar	0.072	0.096	0.253
Coronoid	**0.408**	**0.552**	**0.001**
Condylar	**0.388**	**0.331**	**0.007**
Angular	0.393	0.383	0.245

Significant results at $P = 0.05$ level are highlighted in bold

Table 5

Number of linear distance pairs showing significantly stronger correlations in one species or the other as revealed by MIBoot

Within modules	Angular	Condylar	Incisive	Coronoid
Baboon	2	1	1	0
Mouse	1	1	3	3

Between modules	Condylar-angular	Molar-incisive	Coronoid-angular	Angular-incisive	Condylar-incisive	Angular-molar	Coronoid-molar	Coronoid-incisive	Coronoid-condylar
Baboon	0	3	3	5	3	1	0	0	0
Mouse	1	0	0	0	1	0	2	8	1

Linear distance pairs are characterized as within a particular module or between two modules. Data are shown graphically in Fig. 6

Evol Biol. Author manuscript; available in PMC 2011 December 31.

Table 6

List of heritabilities and their probabilities for baboons and mice for 15 interlandmark distances

Distance	Developmental module	Baboon h^2	Baboon h^2 *P* value	Mouse h^2	Mouse h^2 *P* value
idp to idi	Incisive alveolar	0.0	0.500	0.12 ± 0.04	**1.1×10^{-03}**
sms to idi	Incisive alveolar	0.23 ± 0.09	**0.0003**	0.33 ± 0.06	**2.2×10^{-08}**
sms to idp	Incisive alveolar	0.24 ± 0.11	**0.001**	0.43 ± 0.07	**2.0×10^{-10}**
mpm to iar	Molar alveolar	0.50 ± 0.12	**4.0×10^{-11}**	0.18 ± 0.04	**3.5×10^{-05}**
mpm to ipm	Molar alveolar	0.13 ± 0.09	**0.036**	0.56 ± 0.08	**1.5×10^{-13}**
sms to mpm	Molar alveolar	0.11 ± 0.08	**0.034**	0.25 ± 0.05	**1.2×10^{-06}**
pcp to iar	Coronoid process	0.57 ± 0.13	**7.1×10^{-11}**	0.62 ± 0.08	**3.8×10^{-15}**
pcp to mmn	Coronoid process	0.33 ± 0.10	**7.0×10^{-07}**	0.64 ± 0.08	**1.3×10^{-15}**
mmn to iar	Coronoid process	0.48 ± 0.12	**1.6×10^{-09}**	0.54 ± 0.07	**4.3×10^{-13}**
pmc to amc	Condylar process	0.15 ± 0.11	0.058	0.40 ± 0.07	**7.8×10^{-10}**
mmn to amc	Condylar process	0.26 ± 0.12	**0.002**	0.53 ± 0.07	**7.4×10^{-13}**
pmc to mmn	Condylar process	0.32 ± 0.15	**0.004**	0.54 ± 0.07	**4.7×10^{-13}**
mac to ang	Angular process	0.15 ± 0.11	0.053	0.29 ± 0.06	**2.2×10^{-07}**
ang to irb	Angular process	0.24 ± 0.13	**0.005**	0.44 ± 0.07	**1.4×10^{-10}**
mact to irb	Angular process	0.21 ± 0.10	**0.001**	0.25 ± 0.05	**1.6×10^{-06}**

Significant results are $P = 0.05$ level are highlighted in bold

Table 7

Results from Mantel's tests between genetic correlation matrices of mouse and baboon data with hypothetical matrices for four remaining developmental modules, as well as the average within-module correlation and between-module correlation with significance values for their differences

Developmental module	Baboon				Mouse			
	Mandible *r*	Within-module *r*	Between-module *r*	*P* value	Mandible *r*	Within-module *r*	Between-module *r*	*P* value
All modules	**0.212**	**0.276**	**0.090**	**0.050**	**0.204**	**0.320**	**0.198**	**0.034**
Molar	0.018	0.153	0.113	0.904	−0.004	0.209	0.215	0.984
Coronoid	0.068	0.264	0.109	0.517	0.259	0.627	0.200	0.026
Condylar	**0.184**	**0.517**	**0.100**	**0.078**	**0.003**	**0.219**	**0.214**	**0.988**
Angular	0.026	0.171	0.112	0.793	0.007	0.225	0.214	0.973

Significant or nearly significant correlations and differences in correlations at the $P = 0.05$ level are highlighted in bold

Table 8

Comparison of the variance of the eigenvalues for baboon and mouse genetic correlation matrices for the entire mandible and the five developmental modules

Developmental module	Baboon	Mouse
Whole Mandible	0.100	0.130
Molar	0.199	0.228
Coronoid	0.000	0.669
Condylar	0.460	0.376
Angular	0.337	0.337

Note that there are no associated *P* values as we could not resample the baboon data